THE ASTROPHYSICAL JOURNAL, 518:L65–L68, 1999 June 20

350 MICRON DUST EMISSION FROM HIGH-REDSHIFT OBJECTS

DOMINIC J. BENFORD,[1] PIERRE COX,[2] ALAIN OMONT,[3] THOMAS G. PHILLIPS,[1] AND RICHARD G. MCMAHON[4]
Received 1998 December 28; accepted 1999 April 20; published 1999 May 13

ABSTRACT

We report observations of a sample of high-redshift sources ($1.8 \lesssim z \lesssim 4.7$), mainly radio-quiet quasars, at 350 μm using the bolometer camera SHARC (Submillimeter High Angular Resolution Camera) at the Caltech Submillimeter Observatory. Nine sources were detected ($\gtrsim 4\ \sigma$), and upper limits were obtained for 11 with 350 μm flux density limits (3 σ) in the range 30–125 mJy. Combining published results at other far-infrared and millimeter wavelengths with the present data, we are able to estimate the temperature of the dust, finding relatively low values, averaging 50 K. From the spectral energy distribution, we derive dust masses of a few times $10^8\ h_{100}^{-2}\ M_\odot$ and luminosities of (4–33) $\times\ 10^{12}\ h_{100}^{-2}\ L_\odot$ (uncorrected for any magnification), which imply substantial star formation activity. Thus, both the temperature and dust masses are not very different from those of local ultraluminous infrared galaxies. For this redshift range, the 350 μm observations trace the 60–100 μm rest-frame emission and are thus directly comparable with *IRAS* studies of low-redshift galaxies.

Subject headings: infrared: galaxies — infrared: ISM: continuum — quasars: individual (BR 1202−0725, BRI 1335−0417, 4C 41.17, F10214+472, H1413+117)

1. INTRODUCTION

The study of molecular gas and dust is a significant observational tool for probing the physical conditions and star formation activity in local galaxies. Recent advances in observational techniques at submillimeter and millimeter wavelengths now permit such studies to be made at cosmological distances.

As a result of the *IRAS* survey, many local objects are recognized as containing a large mass of dust and gas, such that the objects may be more luminous in the far-infrared (FIR) than in the optical. The question as to how many such objects there may be at cosmological distances and whether they can account for the recently discovered FIR cosmic background (Puget et al. 1996; Fixsen et al. 1998; Hauser et al. 1998) is attracting much interest and spawning new instrument construction and new surveys (Hughes et al. 1998; Ivison et al. 1998; Kawara et al. 1998; Puget et al. 1999; Barger et al. 1998; Lilly et al. 1999). Existing submillimeter cameras on ground-based telescopes are not yet sensitive and large enough to detect distant objects at 350 μm in arbitrary blank fields, e.g., the initial Caltech Submillimeter Observatory (CSO) Submillimeter High Angular Resolution Camera (SHARC) survey, which achieved 100 mJy (1 σ) over about 10 arcmin^2 (Phillips 1997). However, such cameras can measure the 350 μm flux of objects of known position. A step forward in the field was the recognition of IRAS F10214+4724 as a high-redshift object ($z = 2.286$) by Rowan-Robinson et al. (1991). However, it has proved difficult to find many such objects to study. On the other hand, quasars have sometimes proved to exist in the environs of dusty galaxies (Haas et al. 1998; Lewis et al. 1998; Downes & Solomon 1998). Omont et al. (1996a) have shown by means of a 1300 μm survey of radio-quiet quasars that the dust emission at high redshifts can be detected in a substantial fraction of their project sources.

In this Letter, we present measurements at 350 μm toward a sample of 20 sources, with redshifts $1.8 \lesssim z \lesssim 4.7$, which were selected from different surveys and studies (references are given in Tables 1 and 2). The sources had previously been detected at longer wavelengths and are predominantly from the work of Omont et al. (1996a) and Hughes, Dunlop, & Rawlings (1997). A wavelength of 350 μm roughly corresponds to the peak flux density of highly redshifted ($z \simeq 3$) dust emission of objects with temperatures of 40–60 K. Together with measurements at longer wavelengths, it strongly constrains the dust temperature and, hence, the dust mass and, especially, the luminosity of the object. Some of these results were first presented by Benford et al. (1998). In this Letter, we assume $H_0 = h_{100} \times 100$ km s^{-1} Mpc^{-1} and $\Omega_0 = 1$.

2. OBSERVATIONS AND RESULTS

The measurements were made during a series of observing runs in 1997 February and October and 1998 January and April with the 10.4 m Leighton telescope of the CSO on the summit of Mauna Kea, Hawaii during excellent weather conditions, with 225 GHz atmospheric opacities of $\lesssim 0.05$ (corresponding to an opacity of $\lesssim 1.5$ at 350 μm). We used the CSO bolometer camera SHARC, described by Wang et al. (1996) and Hunter, Benford, & Serabyn (1996). It consists of a linear 24-element close-packed monolithic silicon bolometer array operating at 300 mK. During the observations, only 20 channels were operational. The pixel size is 5″ in the direction of the array and 10″ in the cross direction. The weak continuum sources were observed using the pointed observing mode with the telescope secondary chopping in azimuth by 30″ at a rate of 4 Hz. The telescope was also nodded between the on and the off beams at a rate of ~0.1 Hz. The point-source sensitivity of SHARC at 350 μm is ~1 Jy Hz$^{-1/2}$, and the beam size is ~9″ FWHM. All measurements were made at 350 μm with the exception of H1413+117, which was also observed at 450 μm.

Pointing was checked regularly on nearby strong galactic sources, which also served as secondary calibrators, and was found to be stable with a typical accuracy of $\lesssim 3''$. The planets

[1] California Institute of Technology, MS 320-47, Pasadena, CA 91125.
[2] Institut d'Astrophysique Spatiale, Bât. 121, Université de Paris XI, Orsay, F-91405, France.
[3] Institut d'Astrophysique de Paris, CNRS, 98bis boulevard Arago, Paris, F-75014, France.
[4] Institute of Astronomy, Madingley Road, Cambridge CB3 0HA, England, UK.

TABLE 1

SOURCES DETECTED AT 350 μm AND DERIVED PROPERTIES

Source	z	R.A. (B1950.0)	Decl. (B1950.0)	Flux Density (mJy, $\pm 1\ \sigma$)	$T_{\rm dust}$ (K)	Dust Mass[b] ($10^8\ h_{100}^{-2}\ M_\odot$)	Luminosity[b] ($10^8\ h_{100}^{-2}\ M_\odot$)	References
BR 1202−0725	4.69	12 02 49.3	−07 25 50	106 ± 7	50 ± 7	$4.0^{+0.9}_{-0.8}$	$14.9^{+0.8}_{-0.7}$	1, 2, 3, 4
BRI 1335−0417	4.41	13 35 27.6	−04 17 21	52 ± 8	43 ± 6	$3.6^{+0.5}_{-0.8}$	$6.0^{+0.9}_{-0.5}$	1, 2, 5
HM 0000−263	4.10	00 00 49.5	−26 20 01	134 ± 29	60[a]	$2.0^{+0.2}_{-0.2}$	$20.7^{+1.5}_{-1.5}$	2, 6
4C 41.17	3.80	06 47 20.8	+41 34 04	37 ± 9	52 ± 6	$1.0^{+0.1}_{-0.1}$	$4.3^{+1.4}_{-1.3}$	7, 8
PC 2047+0123	3.80	20 47 50.7	+01 23 56	80 ± 20	50[a]	$2.3^{+0.6}_{-0.6}$	$8.5^{+2.2}_{-1.6}$	9, 10
Q1230+1627	2.74	12 30 39.4	+16 27 26	104 ± 21	49 ± 12	$2.5^{+0.4}_{-0.4}$	$8.2^{+2.0}_{-2.0}$	2, 11
Q0100+1300	2.68	01 00 33.4	+13 00 11	131 ± 28	68 ± 5	$1.2^{+0.5}_{-0.3}$	$23.8^{+0.2}_{-5.8}$	12, 13
H1413+117[b]	2.54	14 13 20.1	+11 43 38	293 ± 14	45 ± 7	$8.9^{+1.9}_{-1.9}$	$17.7^{+1.3}_{-0.6}$	14, 15
F10214+4724[b]	2.28	10 21 31.1	+47 24 23	383 ± 51	55 ± 3	$5.5^{+1.4}_{-1.4}$	$32.8^{+6.5}_{-5.3}$	16

[a] Because of a lack of sufficient data at other wavelengths, the temperatures of these sources are poorly constrained. The available upper limits constrain HM 0000−263 to $50 \lesssim T_{\rm dust} \lesssim 75$ K, so we adopt 60 K; PC 2047+0.123 is essentially unconstrained, so we adopt 50 K since that is roughly the median value for the dust temperature.

[b] The dust masses and luminosities listed above have not been corrected for any lensing amplification. The probable intrinsic values may be found by dividing by $A = 7.6$ for H1413+117 (Alloin et al. 1997) and $A = 13$ for F10214+4724 (Downes, Solomon, & Radford 1995).

REFERENCES.—(1) Storrie-Lombardi et al. 1996; (2) Omont et al. 1996a; (3) McMahon et al. 1994; (4) Isaak et al. 1994; (5) Guilloteau et al. 1997; (6) Schneider, Schmidt, & Gunn 1989; (7) Chambers, Miley, & van Bruegel 1990; (8) Hughes et al. 1997; (9) Schneider, Schmidt, & Gunn 1994; (10) Ivison 1995; (11) Foltz et al. 1987; (12) Steidel & Sargent 1991; (13) Guilloteau et al. 1999; (14) Hazard et al. 1984; (15) Barvainis, Coleman, & Antonucci 1992; (16) Rowan-Robinson et al. 1993.

Mars, Saturn, and Uranus served as primary flux calibrators. The absolute calibration was found to be accurate to within 20%. Repeated observations of H1413+117 and F10214+4724 confirmed a relative flux accuracy of ∼20%. The data were reduced using the CSO BADRS software package. Typical sensitivities (1 σ) of ∼20 mJy were achieved after ∼2500 s of on-source integration time.

Nine sources were detected at levels of 4 σ and above, as outlined in Table 1. Included are the $z > 4$ quasars BR 1202−0725, BRI 1335−0417, and HM 0000−263. Except for the Cloverleaf (H1413+117; Barvainis, Antonucci, & Coleman 1992), the present measurements are the first reported detections for high-redshift quasars at 350 μm. Many of the sources were measured three or more times, providing both consistency checks and improvements in the accuracy of the flux densities. The two strongest sources, H1413+117 and IRAS F10214+4724, were often measured before starting the long (∼2–3 hr) integrations on the weaker sources.

As an illustration of the data quality, Figure 1 shows the 350 μm CSO-SHARC measurement toward BR 1202−0725 at $z = 4.69$. This measurement corresponds to a total of 4 hr integration on source. The source is centered at offset zero. The other channels provide a measure of the neighboring blank-sky emission and a reference for the quality of the detection.

TABLE 2

SOURCES WITH UPPER LIMITS AT 350 μm

Source	z	S_{350} (mJy, $\pm 1\ \sigma$)	$L_{\rm FIR}$ (3 σ) ($10^{12}\ h_{100}^{-2}\ L_\odot$)	References
BR 2237−0607	4.56	5 ± 15	<6	1
BRI 0952−0115	4.43	8 ± 22	<8	1, 2
PSS 0248+1802	4.43	−75 ± 22	<9	3
BR 1117−1329	3.96	27 ± 13	<4	1
Q0302−0019	3.28	34 ± 21	<5	4
Q0636+680	3.18	−123 ± 38	<9	5
Q2231−0015	3.01	−65 ± 24	<6	4
MG 0414+0534	2.64	−24 ± 35	<8	6
Q0050−2523	2.16	69 ± 42	<9	4
Q0842+3431	2.13	16 ± 10	<2	1
Q0838+3555	1.78	39 ± 19	<4	1

REFERENCES.—(1) Omont et al. 1996a; (2) Guilloteau et al. 1999; (3) Kennefick et al. 1995; (4) Hewett, Foltz, & Chaffee 1995; (5) Sargent, Steidel, & Boksenberg 1989; (6) Barvainis et al. 1998.

Eleven sources with redshifts between 1.8 and 4.5 were not detected at 350 μm, with flux density upper limits at the 3 σ level of 30–125 mJy. Table 2 lists their names, redshifts, 350 μm flux density measurements with $\pm 1\ \sigma$ errors, and a 3 σ upper limit to their luminosities (see below).

3. DISCUSSION

Figure 2 displays the spectral energy distributions of the six sources detected at 350 μm for which fluxes at two or more other wavelengths are available from the literature. In the following, we will first comment on individual sources and then discuss the physical properties of the objects.

The two radio-quiet, $z > 4$ quasars BR 1202−0725 and BRI 1335−0417 are exceptional objects with large masses of gas (∼$10^{11}\ M_\odot$), and they have been detected in CO by Omont et al. (1996b) and Guilloteau et al. (1997). They both are clearly detected at 350 μm with flux densities of 106 ± 7 and 52 ± 8 mJy, respectively. However, BRI 0952−0115, which is the third $z > 4$ quasar in which CO has been measured (Guilloteau

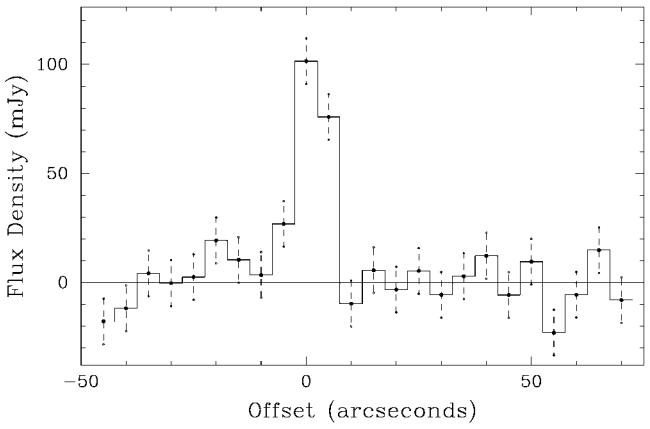

FIG. 1.—The 350 μm flux density measured in the bolometers of the SHARC array toward BR 1202−0725 at $z = 4.69$. Offsets are given in arcseconds with respect to the reference channel number 10. The source is centered at offset zero. Emission is also seen in the two neighboring pixels because the bolometers sample the diffraction pattern of the telescope with a Nyquist sampling.

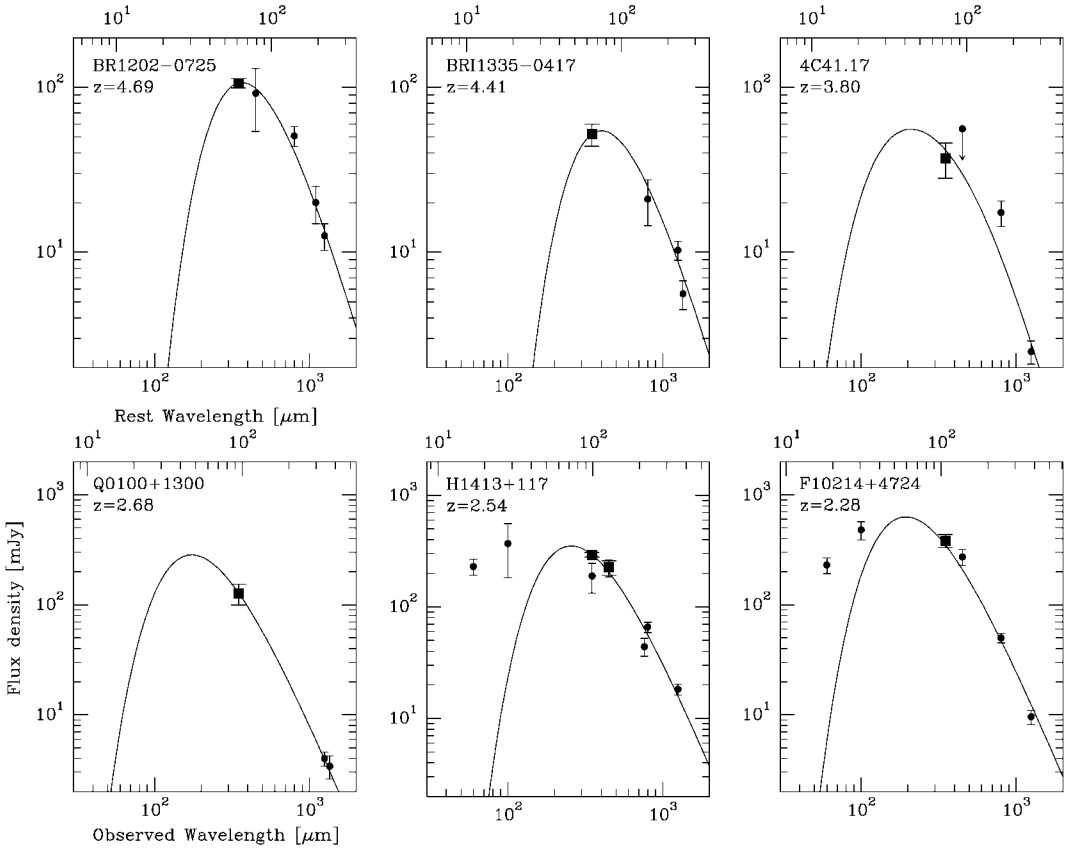

FIG. 2.—Spectral energy distributions of six of the high-redshift objects discussed in this Letter. The 350 μm fluxes, shown as squares, are the measurements made with SHARC at the CSO. Fluxes taken from the literature (references 2, 3, 4, 5, 8, 10, 13, 15, and 16 from Table 1) are shown as circles. The observed fluxes at $\lambda_{obs} \geq 350$ μm were approximated by graybody spectra (*solid lines*), assuming an emissivity index $\beta = 1.5$. The dust temperature results from a nonlinear least-squares fit to the data (see text).

et al. 1999), is not detected at 350 μm at a 3 σ level of 65 mJy. This upper limit is consistent with the weak flux density of BRI 0952−0115 at 1.3 mm, 2.8 ± mJy (Omont et al. 1996a; Guilloteau et al. 1999), and a temperature of ~50 K (see below). The radio-quiet quasar HM 0000−263 at $z = 4.11$, which was not detected at 1.25 mm using the 30 m telescope because of its low declination (Omont et al. 1996a), shows a large flux density at 350 μm (134 ± 29 mJy). Measurements at other wavelengths would be useful to further constrain the properties of this object.

The detection of the $z = 3.8$ radio galaxy 4C 41.17 with a flux density of 37 ± 9 mJy at 350 μm is one of the most sensitive measurements of this study. This sensitivity was reached after only 45 minutes of on-source time and defines the limits that can be achieved with SHARC in the pointed observing mode under excellent weather conditions. A marginal detection (4 σ) was achieved at 350 μm of PC 2047+0123, a $z = 3.80$ quasar studied by Ivison (1995). Finally, the 350 μm flux density of the Cloverleaf (H1413+117) is significantly higher than the value published by Barvainis et al. (1992), i.e., 293 ± 14 mJy as compared to 189 ± 56 mJy. We have also obtained for the Cloverleaf a 450 μm flux density of 226 ± 34 mJy, in excellent agreement with the measurement of 224 ± 38 mJy at 438 μm of Barvainis et al. (1992), as shown in Figure 2.

A graybody was fit to the data points S_ν for wavelengths of 350 μm and longward, as a function of the rest frequency $\nu = \nu_{obs}/(1 + z)$, of the form

$$S_\nu = B_\nu \Omega [1 - \exp(-\tau)] \quad \text{with } \tau = (\nu/\nu_0)^\beta, \tag{1}$$

where $\nu_0 = 2.4$ THz is the critical frequency at which the source becomes optically thin and Ω is the solid angle of emission. The shape of the fitted graybody is very weakly dependent on the value of ν_0 (Hughes et al. 1993). The data were each weighted by their statistical errors in the χ^2 minimization. This yields the dust temperature, dust mass (following Hildebrand 1983, using a dust mass emission coefficient at ν_0 of 1.9 m^2 kg^{-1}), and luminosity of the sources. When β is considered as a free parameter, we find that the average value of β is 1.5 ± 0.2 for the detected sources. The fits shown in Figure 2 assume an emissivity index of $\beta = 1.5$. We estimated the 1 σ uncertainty in the temperature by examining the χ^2_ν hypersurface in the range $1 \leq \beta \leq 2$, similar to the method of Hughes et al. (1993). To evaluate the uncertainties associated with the mass and luminosity derived from the fitted temperature and $\beta = 1.5$, we used the maximum and minimum values of the mass and luminosity, which are compatible with the data plus or minus the statistical error. No lensing amplification was taken into account. The temperature, dust mass, and luminosities derived under these assumptions are given in Table 1. Two of the sources with upper limits have 1.25 mm detections (Omont et al. 1996a), which, together with the 350 μm data, yields an upper limit to their temperature. For Q0842+3431, we find

that $T_{\rm dust} < 40$ K, while for BR 1117−1329 a limit of $T_{\rm dust} < 60$ K is found. If the dust is at the temperature limit, these quasars have dust masses less than $10^8\ M_\odot$. For the other sources, an estimate of the maximum luminosity has been given under the assumption that each object has a temperature of 50 K and an emissivity index of $\beta = 1.5$.

The total luminosity is probably underestimated, since a large luminosity contribution from higher temperature dust cannot be ruled out for most sources. However, in the case of H1413+117 and IRAS F10214+4724, the available *IRAS* data allow us to fit an additional warm component. For IRAS F10214+4724, the cold component model carries roughly 60% of the total luminosity; in the case of H1413+117, which has a hotter mid-IR spectrum, the total luminosity is underestimated by a factor of 3. Under the assumption that the majority of the luminosity is carried by the cold component (Table 1), the median luminosity-to-mass ratio is around $100\ L_\odot/M_\odot$, assuming a gas-to-dust ratio of ∼500, similar to that of IRAS F10214+4724 and H1413+117 (Downes et al. 1992; Barvainis et al. 1995) or of ultraluminous infrared galaxies, i.e., 540 ± 290 (Sanders, Scoville, & Soifer 1991).

The peak emission in the rest frame is found to be in the wavelength range $\lambda_{\rm peak} \sim 60$–$80\ \mu$m (Fig. 2), implying dust temperatures of 40–60 K (Table 1). These temperatures are nearly a factor of 2 lower than previously estimated for ultraluminous sources (e.g., Chini & Krügel 1994). If the temperature range we find is typical for the cold component of highly redshifted objects, multiband photometric studies in the submillimeter/FIR, such as planned with the Far-Infrared and Submillimeter Telescope, will provide reasonably accurate redshift estimates for the sources detected in deep-field surveys.

The global star formation rate in each of the detected sources can be estimated using the relation of Thronson & Telesco (1986): $\mathrm{SFR} \sim \Psi\ 10^{-10} L_{\rm FIR}/L_\odot h_{100}^{-2}\ M_\odot\ \mathrm{yr}^{-1}$, with $\Psi \sim 0.8$–2.1. For our mean luminosity of $1.7 \times 10^{13}\ h_{100}^{-2}\ L_\odot$, this yields an SFR of $\sim$2000 $M_\odot\ h_{100}^{-2}\ \mathrm{yr}^{-1}$ (uncorrected for lensing) if all the submillimeter flux is from a starburst component. If we assume a final stellar mass of $\sim 2 \times 10^{12}\ M_\odot$, a value appropriate to a giant elliptical like M87 (Okazaki & Inagaki 1984), then the timescale for formation in a single massive starburst is $\simeq 10^9\ h_{100}^2$ yr. Given the large mass of dust already present in these quasars, a substantial amount of this star formation must already have occurred. For the most distant quasars, for which the age of the universe is similar to the derived formation timescale, this implies a very high redshift ($z \gtrsim 5$) for the era of initial star formation, in agreement with models of high-redshift Lyα emitters (Haiman & Spaans 1999).

The CSO is funded by the NSF under contract AST 96-15025. We thank T. R. Hunter for help with the fitting/derivation programming and D. Downes for helpful comments. P. C. acknowledges financial support from Institut National des Sciences de l'Univers (Programmes Grands Télescopes Etrangers) and Physique et Chimie du Milieu Interstellaire.

REFERENCES

Alloin, D., Guilloteau, S., Barvainis, R., & Tacconi, L. 1997, A&A, 321, 24
Barger, A. J., Cowie, L. L., Sanders, D. B., Fulton, E., Taniguchi, Y., Sato, Y., Kawara, K., & Okuda, H. 1998, Nature, 394, 248
Barvainis, R., Alloin, D., Guilloteau, S., & Antonucci, R. 1998, ApJ, 492, L13
Barvainis, R., Antonucci, R., & Coleman, P. 1992, ApJ, 399, L19
Barvainis, R., Antonucci, R., Hurt, T., Coleman, P., & Reuter, H.-P. 1995, ApJ, 451, L9
Benford, D. J., Cox, P., Omont, A., & Phillips, T. G. 1998, BAAS, 192, 11.04
Chambers, K. C., Miley, G. K., & van Breugel, W. J. M. 1990, ApJ, 363, 21
Chini, R., & Krügel, E. 1994, A&A, 288, L33
Downes, D., Radford, S. J. E., Greve, A., Thum, C., Solomon, P. M., & Wink, J. E. 1992, ApJ, 398, L25
Downes, D., & Solomon, P. M. 1998, ApJ, 507, 615
Downes, D., Solomon, P. M., & Radford, S. J. E. 1995, ApJ, 453, L65
Fixsen, D. J., Dwek, E., Mather, J. C., Bennett, C. L., & Shafer, R. A. 1998, ApJ, 508, 123
Foltz, C. B., Chaffee, F. H., Hewett, P. C., McAlpine, G. M., Turnsheck, D. A., Weymann, R. J., & Anderson, S. F. 1987, AJ, 94, 1423
Guilloteau, S., Omont, A., McMahon, R. G., Cox, P., & Petitjean, P. 1997, A&A, 328, L1
———. 1999, A&A, in press
Haas, M., Chini, R., Meisenheimer, K., Stickel, M., Lemke, D., Klaas, U., & Kreysa, E. 1998, ApJ, 503, L109
Haiman, Z., & Spaans, M. 1999, ApJ, in press (astro-ph/9809223)
Hauser, M. G., et al. 1998, ApJ, 508, 25
Hazard, C., Morton, D. C., Terlevich, R., & McMahon, R. G. 1984, ApJ, 282, 33
Hewett, P. C., Foltz, C. B., & Chaffee, F. H. 1995, AJ, 109, 1498
Hildebrand, R. H. 1983, QJRAS, 24, 267
Hughes, D. H., Dunlop, J. S., & Rawlings, S. 1997, MNRAS, 289, 766
Hughes, D. H., Robson, E. I., Dunlop, J. S., & Gear, W. K. 1993, MNRAS, 263, 607
Hughes, D. H., et al. 1998, Nature, 394, 241
Hunter, T. R., Benford, D. J., & Serabyn, E. 1996, PASP, 108, 1042
Isaak, K. G., McMahon, R. G., Hills, R. E., & Withington, S. 1994, MNRAS, 269, L28
Ivison, R. J. 1995, MNRAS, 275, L33
Ivison, R. J., Smail, I., Le Borgne, J.-F., Blain, A. W., Kneib, J.-P., Bézecourt, J., Kerr, T. H., & Davies, J. K. 1998, MNRAS, 298, 583
Kawara, K., et al. 1998, A&A, 336, L9
Kennefick, J. D., De Carvalho, R. R., Djorgovski, S. G., Wilber, M. M., Dickson, E. S., Weir, N., Fayyad, U., & Roden, J. 1995, AJ, 110, 78
Lewis, G. F., Chapman, S. C., Ibata, R. A., Irwin, M. J., & Totten, E. J. 1998, ApJ, 505, L1
Lilly, S. J., Eales, S. A., Gear, W. K. P., Hammer, F., Le Fèvre, O., Crampton, D., Bond, J. R., & Dunne, L. 1999, ApJ, in press (astro-ph/9901047)
McMahon, R. G., Omont, A., Bergeron, J., Kreysa, E., & Haslam, C. G. T. 1994, MNRAS, 267, L9
Okazaki, A. T., & Inagaki, S. 1984, PASJ, 36, 17
Omont, A., McMahon, R. G., Cox, P., Kreysa, E., Bergeron, J., Pajot, F., & Storrie-Lombardi, L. J. 1996a, A&A, 315, 1
Omont, A., Petitjean, P., Guilloteau, S., McMahon, R. G., Solomon, P. M., & Pécontal, E. 1996b, Nature, 382, 428
Phillips, T. G. 1997, in The Far-Infrared and Submillimetre Universe, ed. A. Wilson (ESA SP-401; Noordwijk: ESA), 223
Puget, J.-L., Abergel, A., Bernard, J.-P., Boulanger, F., Burton, W. B., Desert, F.-X., & Hartmann, D. 1996, A&A, 308, L5
Puget, J.-L., et al. 1999, A&A, 345, 29
Rowan-Robinson, M., et al. 1991, Nature, 351, 719
———. 1993, MNRAS, 261, 513
Sanders, D. B., Scoville, N. Z., & Soifer, B. T. 1991, ApJ, 370, 158
Sargent, W. L. W., Steidel, C., & Boksenberg, A. 1989, ApJS, 69, 703
Schneider, D. P., Schmidt, M., & Gunn, J. 1989, AJ, 98, 1507
———. 1994, AJ, 107, 1245
Steidel, C. C., & Sargent, W. L. W. 1991, ApJ, 382, 433
Storrie-Lombardi, L. J., McMahon, R. G., Irwin, M. J., & Hazard, C. 1996, ApJ, 468, 121
Thronson, H., & Telesco, C. 1986, ApJ, 311, 98
Wang, N., et al. 1996, Appl. Opt., 35, 6629